Peripapillary vessel density and retinal nerve fiber layer thickness changes in early diabetes retinopathy

Xiang–Ning Wang[1], Xuan Cai[1], Ting–Ting Li[1], Da Long[1], Qiang Wu[1,2]

[1]Department of Ophthalmology, Shanghai Jiao Tong University Affiliated Sixth People's Hospital, Shanghai 200233, China
[2]Shanghai Key Laboratory of Diabetes Mellitus, Shanghai 200233, China
Correspondence to: Qiang Wu. Department of Ophthalmology, Shanghai Jiao Tong University Affiliated Sixth People's Hospital, No.600 Yishan Road, Xuhui District, Shanghai 200233, China. qiang.wu@shsmu.edu.cn.

Abstract

● **AIM:** To perform a quantitative analysis of the peripapillary vessel density (VD) and retinal nerve fiber layer (RNFL) thickness changes in patients with early stage of diabetic retinopathy (DR).

● **METHODS:** In this case-control study, swept-source optical coherence tomography angiography (SS-OCTA) imaging was used to examine diabetic and age-matched healthy subjects. The optic disc HD 6×6 mm^2 blood flow imaging scan mode was selected. Automatic software was used to measure the peripapillary VD, capillary vessel density (CVD), and RNLF in an optic nerve head (ONH) filed based on the Garway-Heath map. In addition, the correlation between peripapillary VD, CVD, and RNFL was further investigated.

● **RESULTS:** The cohort consisted of 32 healthy individuals and 72 patients with diabetes (34 eyes with no DR and 38 eyes with mild-moderate NPDR). Peripapillary VD decreased in the mild-moderate NPDR group compared to the control group in most regions ($P<0.05$). Peripapillary CVD and RNFL thickness were significantly lower in the mild-moderate NPDR group in the superior temporal (ST) quadrants ($P=0.018$, $P=0.030$). In the correlation analysis of each region, the RNFL thickness in the NS region was positively correlated with the peripapillary VD and CVD ($r=0.233$, $P=0.05$; $r=0.288$, $P=0.015$). In the TI region, the RNFL thickness was positively correlated with the peripapillary CVD ($r=0.237$, $P=0.047$).

● **CONCLUSION:** The measurement based on the ONH topographic map may be helpful in detecting functional and structural impairments in DR. The peripapillary VD, CVD and RNFL decrease in early DR, and the RNFL thickness altered in association with the CVD or/and VD in some regions.

● **KEYWORDS:** vessel density; retinal nerve fiber layer; diabetic retinopathy; OCTA; swept-source

INTRODUCTION

Diabetic retinopathy (DR) is a potentially fatal complication with diabetes mellitus (DM) and the primary cause of blindness worldwide[1]. Previous studies have shown that early diagnosis of type 2 diabetes mellitus (T2DM) and screening for retinopathy is associated with a lower incidence and severity of retinopathy[2]. However, when retinal lesions become clinically evident, it is impossible to reverse the injury, and the likelihood of DR progression increases[3-4]. The present DR management is focused on the late stages, where retinal systems and vision acuity have also been compromised[5]. Thus, understanding the pathogenesis of neurovascular impairments could lead to novel and efficient preventive strategies. As a result, diagnosis and tracking slight neurovascular changes that are in the early stages of DR are essential.

Recent studies on DR pathogenesis found that neuronal dysfunction and neurodegeneration are closely associated with microvascular dysfunction and that neurovascular unit degeneration could be regarded as an essential component of DR pathology[6-9]. In addition, evidence from diabetic donors' and diabetic animal models' retinas demonstrated that retinal neuronal cell degeneration or apoptosis develops early in diabetes[10-12].

Of these neuronal modifications, the thinning of the retinal nerve fiber layer (RNFL) is an essential feature of the inner retinal layers and is speculated as to the earliest improvement in DR neurodegenerative lesions. RNFL loss leads to defects in various ophthalmological tests, including electroretinograms, contrast sensitivity, dark adaptation, and microperimetry.

Optical coherence tomography angiography (OCT-A) is a non-invasive and reproducible imaging procedure that was recently used to study macular and peripapillary vascular structures with unlikely details and clarification[13-14]. Early variations in the peripapillary vessel anatomy and vessel density (VD) of the radial peripapillary plexus have been linked to RNFL thinning in patients with DM but without DR[15].

The new technique, swept-source OCT (SS-OCT), improves the imaging depth and scanning speed that facilitates anterior segment assessment with corneal graft inspection, *i.e.*, it allows a precise qualitative and quantitative assessment of vascular improvements in the fundus and presents various application prospects. Additionally, Garway-Heath *et al*[16] constructed a clinical map that relates visual field test points to the regions of the optic nerve head (ONH). The map is valuable in the clinical diagnosis of glaucoma patients and suspects and the research of the connection between retinal light sensitivity and ONH structure. Therefore, we used swept-source optical coherence tomography angiography (SS-OCTA) technology and Garway-Heath map-based ONH measurement software to explore the peripapillary VD, capillary vessel density (CVD), and RNFL thickness changes in early DR.

SUBJECTS AND METHODS

Ethical Approval The study was approved by the Shanghai Sixth People's Hospital Institutional Review Board. All the protocols followed the principles of Helsinki Declaration, and informed consent was obtained prior to participation in the study. The study was registered in the Chinese clinical trial registry (http://www.chictr.org.cn/, Registration number: ChiCTR1900028607). Between October 2020 and March 2021, diabetic patients were recruited from the Shanghai Diabetes Center at the Shanghai Sixth People's Hospital Affiliated University. Healthy adults were recruited from the same hospital at the same time.

All participants underwent ophthalmological analysis, including health history, visual acuity evaluation, biomicroscopy of the anterior segment using a slit lamp, ophthalmoscopy of the posterior segment, wide-field color fundus photography using Optos California (Optos plc, Dunfermline, UK), and Spectralis SD-OCT scans (Spectralis HRA+OCT; Heidelberg Engineering, Heidelberg, Germany). Based on the wide-field color fundus photography and the International Clinical Diabetic Retinopathy Disease Severity Scale[17], two senior graders (Long D and Cai X) graded each subject's DR as no DR, mild to moderate, or severe non-proliferative diabetic retinopathy (NPDR), or proliferative diabetic retinopathy (PDR). Each subject had one eye chosen as the research object, and if both eyes matched the eligibility criteria, the eye with higher visual acuity or a lower refractive error was chosen. All the participants were at least 18-year-old, had a logMAR visual

acuity of at least 0.5 log units, and a refractive error of no more than -3.00 diopters (D) or +3 D-equivalent spheres. The exclusion criteria were as follows: 1) unable to give informed consent or consent to a full examination; 2) glaucoma, cup/disc (C/D)>0.4, or intraocular pressure >21 mm Hg; 3) pregnant or nursing; 4) active eye infections (such as blepharitis, keratitis, scleritis, conjunctivitis, *etc.*); 5) history of ocular disorders that affecting the neural and vascular structures of the eye (ocular trauma, amblyopia, retinal vein occlusion, retinal detachment, macular disease, multiple sclerosis, Alzheimer disease, hypertensive retinopathy, *etc.*), and history of ocular procedures other than cataract surgery (laser, intravitreal injections, and vitreoretinal surgery); 6) degree of DR classification greater than moderate NPDR; 7) presence of diabetic macular edema (DME).

SS-OCT/OCTA Image Acquisition and Analysis The SS-OCT/OCTA device was designed for the central wavelength laser (VG200S; SVision Imager, Henan, China) of 1050 nm with a scan rate of 200 000 A-scans/s. The device was equipped with an eye monitoring tool based on an integrated confocal laser ophthalmoscope for the removal of objects of eye movement. The axial and lateral resolutions were 5 and 13 μm, respectively. The depth of the scan was 3 mm.

The tomography/OCTA volumes of optical coherence were obtained covering a 6×6 mm^2 retinal region and were based on the optic disk. Every volume of 6×6 mm^2 consisted of 512A scans for the B-scan (24 mm space between adjacent A-shapes) and 512B-scan spaces for scanning by voltage (24 mm spaces between adjacent B-shapes). To detect the motion contrast for OCTA, the optical microangiography (OMAGC) algorithm was used. Both OCTA photography was carried out by professional ophthalmic photographers, who, if possible, repeated the image acquisition to ensure photographs with intense OCT signal penetration and minimal motion artifacts. Scans with an signal-to-noise ratio (SNR) >8 decibels (dB) were considered good quality. The quality ratings for the scans were expressed as SNR in dB over a spectrum of 1 (poor quality) to 10 (excellent quality). Only photographs with a score of ≥8 were considered.

Image Analysis The ONH program installed in the machine assessed the data automatically. The ONH was a 4 mm diameter ring. The middle was a 2 mm circle, and the 2-4 mm circle was separated using nerve fiber flux (NFF) cartographies in eight areas (Garway-Heath *et al*[16] scheme). The eight regions include nasal superior (NS), nasal inferior (NI), inferior nasal (IN), inferior temporal (IT), temporal inferior (TI), temporal superior (TS), superior temporal (ST), and superior nasal (SN). The built-in program was utilized to assess each pattern of the average retinal VD of the inner retina (from ILM-5 mm to IPL/INL+(INL/OPL-IPL/INL)/2) was measured

(version1.31.6; VG200D, SVision Imaging Ltd, Henan Province, China). The density of peripapillary CVD was then calculated using the procedure of removing massive blood vessels. Simultaneously, the corresponding RNFL thickness was also calculated (Figure 1).

Statistical Analysis All data analyses were carried out using the SPSS version 19.0 program (IBM Co., Chicago, IL, USA). The data are presented as the mean±standard deviation (SD) for continuous and categorical variables. One-way variation analysis (ANOVA) was conducted to compare the continuous variables with Bonferroni post hoc tests, independent t-test or Mann-Whitney U test. χ^2 test was used to compare the proportions between groups. Pearson's correlation and multivariable linear regression analysis investigated the correlation between retinal neurodegeneration and intrinsic risk factors. The two-tailed P-values were recorded. To evaluate statistical significance, a 0.05-type I error level was used.

RESULTS

Patient Characteristics Based on the inclusion/exclusion criteria, the study included 104 participants (32 controls on health and 72 diabetes patients; 45 males and 59 females), of which 32 comprised the control group, 34 were T2DM without DR (no-DR group), and 38 were mild-moderate DR. The sample participants' demographic characteristics are summarized in Table 1.

The mean age of the subjects in the three groups was 57.46±9.39y, 63.59±9.69y, and 58.15±10.38y, respectively; the difference was significant among the groups (P=0.112; Table 1). No statistically significant differences were identified in patients' sex (P=0.953), laterality (P=0.734), visual acuity (P=0.421), and mean spherical equivalent (P=0.685) among three groups. Among the diabetic patients, the comparison [duration of diabetes, fasting blood glucose (FBG), hemoglobin A1c (HbA1c), and glycated albumin] showed that only FBG was significantly different between the mild-moderate NPDR and no-DR groups (t=-2.004, P=0.049).

Repeatability The repeatability test was carried out for 12 patients with a mean (SD) age of 59.46±6.24 (range: 50-74)y. Among these participants, six had diabetes. The intraclass correlation coefficient (ICC) scores were 0.89 for VD, 0.91 for CVD, and 0.92 for RNFL.

Quantitative Analysis In order to analyze the VD quantitatively in different regions, non-parametric Kruskal-Wallis with Bonferroni's post hoc test was applied. The statistical results are displayed in Table 2 and Figure 2. In the central ring, the mean VD of the control, no-DR, and mild-moderate NPDR groups was 47.54±8.23, 46.01±9.17, 48.93±9.84, with no significant differences between the groups (P=0.466). In the 2-4 mm circle, significant differences were detected among the three groups (P=0.006). VD in the no-DR and mild-moderate
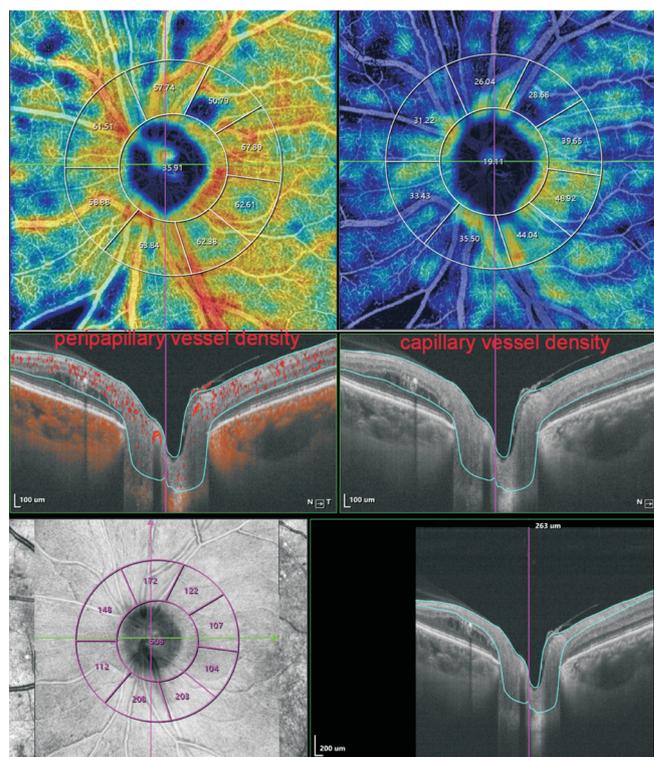
Figure 1 The swept-source optical coherence tomography angiography technology and Garway-Heath map-based ONH measurement software were applied to explore the peripapillary vessel density, capillary vessel density and retinal nerve fiber layer thickness.

Table 1 Demographic and clinical characteristics of the study participants

Characteristics	Control	No-DR	Mild DR	P
Number	32	34	38	-
Age, y	57.46±9.39	63.59±9.69	58.15±10.38	0.112[a]
Gender (male/female)	14/18	14/20	17/21	0.953[b]
Laterality (right/left)	20/12	18/16	22/16	0.734[b]
Visual acuity, logMAR	0.16±0.24	0.11±0.19	0.12±0.21	0.421[a]
Refractive error, diopters	-0.29±1.07	-0.04±1.18	-0.48±1.05	0.685[a]
Duration of diabetes, y	-	12.52±8.64	13.14±6.17	0.733[c]
FBG, mmol/L	-	6.65±1.28	7.46±1.55	0.049[c]
HbA1c, %		7.53±1.34	8.12±1.36	0.345[c]
Glycated albumin, %		16.74±5.84	14.84±7.06	0.428[c]

Data are as mean±standard deviation. [a]One-way analysis of variance; [b]Chi-square Tables test; [c]Independent samples t-test. FBG: Fasting blood glucose; DR: Diabetic retinopathy; HbA1c: Hemoglobin A1c.

NPDR groups was significantly lower than that in the normal group, but no significant difference was observed between the no-DR and mild-moderate NPDR groups. In the eight regions of 2-4-mm circle, differences were observed in the superior, inferior, NS, and IN quadrants (P=0.007, 0.026, 0.007, and 0.039). Among these, the VD of the mild-moderate NPDR group was lower than that of the control group (P<0.05); however, the difference between the mild-moderate NPDR vs
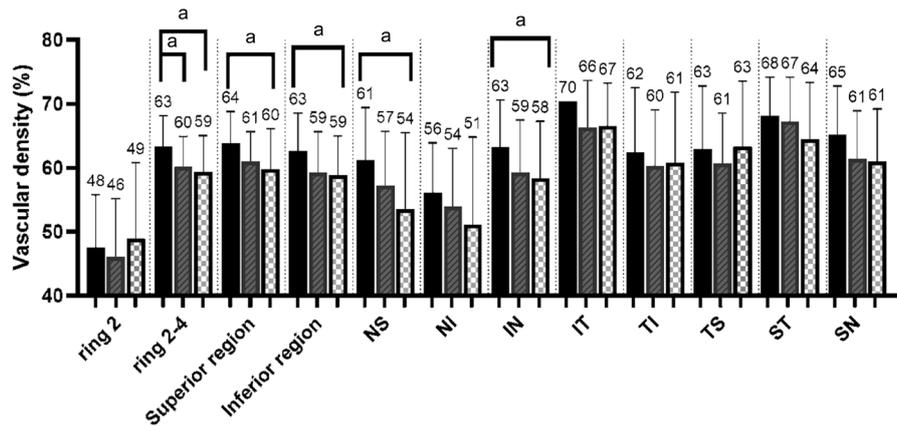
Figure 2 Comparison of vessel density in different groups in optic nerve head grid [a]*P*<0.05. NS: Nasal superior; NI: Nasal inferior; IN: Inferior nasal; IT: Inferior temporal; TI: Temporal inferior; TS: Temporal superior; ST: Superior temporal; SN: Superior nasal.

Table 2 Comparison of perfusion area parameters between each group mean±SD

Classification	VD			CVD			RNFL		
	Control group	No-DR	Mild-moderate DR	Control group	No-DR	Mild-moderate DR	Control group	No-DR	Mild-moderate DR
2 mm	47.54±8.23	46.01±9.17	48.93±9.84	25.54±5.74	24.98±6.28	26.37±5.79	408.61±40.06	399.39±48.48	392.98±40.66
2-4 mm	63.27±4.88	60.12±4.80	59.31±5.75[a]	35.37±3.98	34.62±7.93	32.20±5.71	126.28±17.10	125.88±15.26	116.74±16.45
S	63.88±4.94	60.97±4.68	59.77±6.33[a]	35.56±4.11	35.25±7.96	32.62±6.06	126.87±22.44	123.71±15.13	113.26±17.52
I	62.61±5.98	59.20±6.44	58.81±6.19[a]	34.94±5.39	33.94±6.29	31.74±6.16	125.64±16.28	128.26±18.62	119.46±20.73
NS	61.15±8.25	57.23±8.48	53.51±8.01[a]	29.70±5.16	29.29±6.69	25.56±6.97	106.38±22.80	109.75±19.01	97.83±23.72
NI	56.38±7.46	53.90±9.15	51.13±9.68	28.36±5.49	27.79±6.59	24.46±8.94	84.85±14.71	88.93±14.21	85.31±17.66
IN	63.26±7.35	59.24±8.23	58.35±8.91[a]	32.58±7.21	32.23±7.95	30.77±8.36	142.04±30.37	147.35±33.59	144.76±32.39
IT	70.41±9.12	66.28±7.39	66.52±6.73	44.01±8.94	41.80±8.52	39.04±9.81	178.47±32.47	182.76±29.70	169.37±30.76
TI	62.37±8.13	60.29±8.80	60.76±9.07	37.64±6.33	36.46±8.55	35.36±7.78	107.38±13.21	103.07±18.81	91.52±19.48
TS	62.89±9.91	60.62±7.95	63.33±8.43	38.99±4.88	38.03±7.66	38.15±7.13	98.95±13.40	100.14±16.87	95.01±16.75
ST	68.14±6.04	67.26±6.91	64.46±8.89	42.63±8.58	41.38±6.18	37.27±8.08[a]	163.56±20.21	147.95±20.82	137.32±25.73[a]
SN	65.19±7.58	61.39±7.51	60.96±8.26	35.55±6.89	34.78±8.01	34.49±8.38	153.43±37.09	146.94±34.33	134.83±33.24

[a]One-way analysis of variance followed by Bonferroni post-hoc tests. DR: Diabetic retinopathy; VD: Vessel density; CVD: Capillary vessel density; RNFL: Retinal nerve fiber layer; S: Superior; I: Inferior; NS: Nasal superior; NI: Nasal inferior; IN: Inferior nasal; IT: Inferior temporal; TI: Temporal inferior; TS: Temporal superior; ST: Superior temporal; SN: Superior nasal.

no-DR and no-DR *vs* control groups were not significant (*P*>0.05).

Furthermore, we estimated the changes in peripapillary CVD after removing large blood vessels. The sectored analyses of each CVD in the ONH grid are shown in Table 2 and Figure 3. In the 2-4 mm circle, the mean CVD did not differ significantly among the control, no-DR, and mild-moderate NPDR groups (*P*=0.117). In the eight regions of the 2-4 mm circle, no significant differences were detected in the ST quadrants (*P*=0.018). In addition, the CVD of the mild-moderate NPDR group decreased significantly compared to the control group (*P*<0.05).

A similar finding was observed in RNFL. The RNFL thickness did not differ significantly in mild-moderate NPDR *vs* no-DR and no-DR *vs* control groups (*P*>0.05). However, the RNFL thickness in the mild-moderate NPDR group was significantly lower than that in the control group in the ST quadrants (*P*=0.030; Table 2 and Figure 4).

Pearson's correlation analysis was used to calculate the correlation between RNFL thickness and peripapillary VD and CVD (Table 3 and Figure 5). Furthermore, in diabetic patients, the average RNFL thickness and the mean peripapillary VD and CVD were positively correlated but not significantly (*r*=0.141, *P*=0.240; *r*=0.175, *P*=0.145). In the correlation analysis of each region, the RNFL thickness in the NS region was positively correlated with peripapillary VD and CVD (*r*=0.233, *P*=0.05; *r*=0.288, *P*=0.015; Table 3), while in the TI region, the RNFL thickness was positively correlated with peripapillary CVD (*r*=0.237, *P*=0.047; Table 3).

DISCUSSION

This study was based on the Garway-Heath map to explore the changes in peripapillary VD, CVD, and RNFL thickness in the early stage of DR. Consequently, we found that functional and structural impairments had already begun in the early stages of DR. Correlation research analysis demonstrated a correlation between neural and vascular structures.
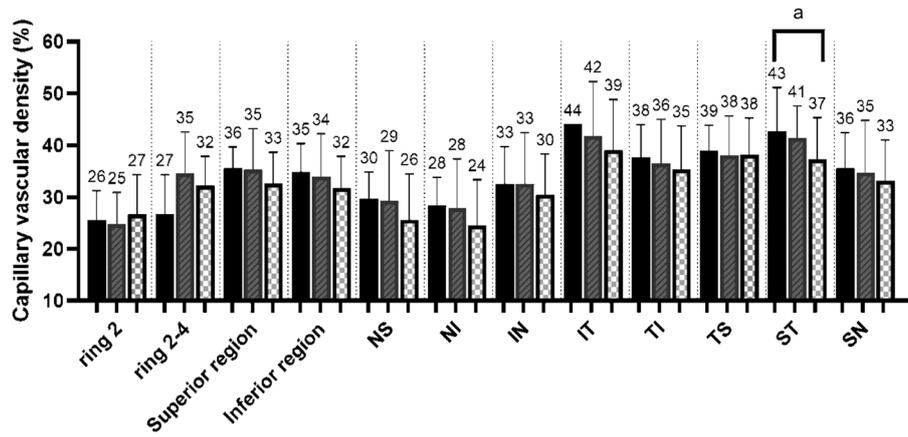
Figure 3 Comparison of capillary vessel density in different groups in ONH grid [a]*P*<0.05 indicates a significant difference. ONH: Optic nerve head. NS: Nasal superior; NI: Nasal inferior; IN: Inferior nasal; IT: Inferior temporal; TI: Temporal inferior; TS: Temporal superior; ST: Superior temporal; SN: Superior nasal.
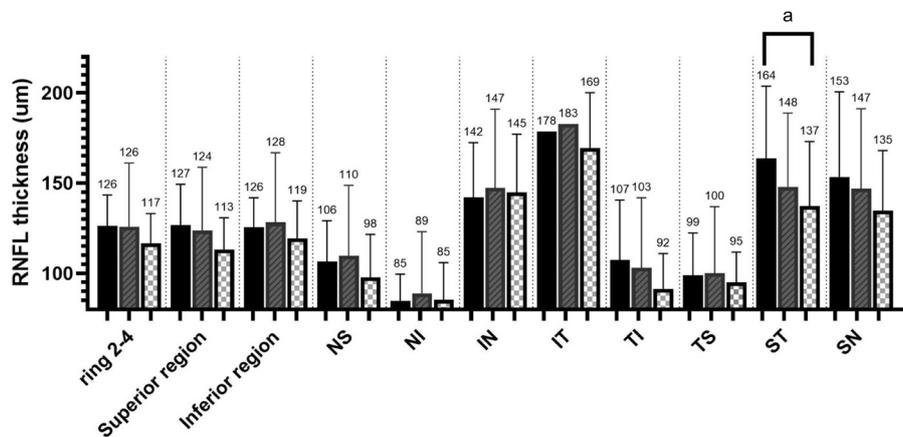
Figure 4 Comparison of peripapillary retinal nerve fiber layer in different groups in ONH grid [a]*P*<0.05. ONH: Optic nerve head. NS: Nasal superior; NI: Nasal inferior; IN: Inferior nasal; IT: Inferior temporal; TI: Temporal inferior; TS: Temporal superior; ST: Superior temporal; SN: Superior nasal.
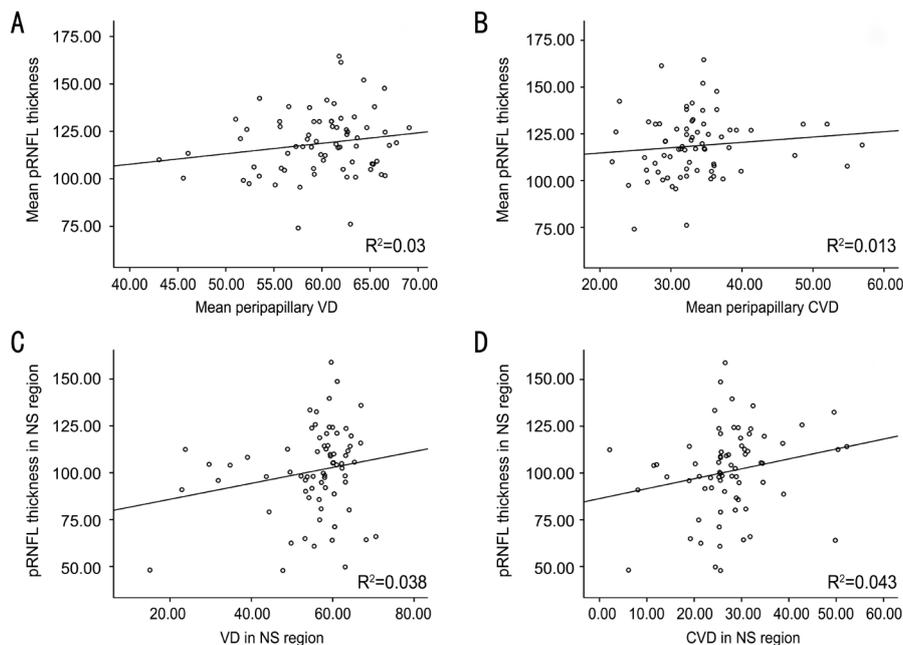
Figure 5 Pearson's correlation analysis between RNFL thickness and peripapillary VD and CVD The average RNFL thickness and the mean peripapillary VD and CVD were positively correlated but not significantly (*r*=0.141, *P*=0.240; *r*=0.175, *P*=0.145; A, B). In the correlation analysis of each region, the RNFL thickness in the NS region was positively correlated with peripapillary VD and CVD (*r*=0.233, *P*=0.05; *r*=0.288, *P*=0.015; C, D). VD: Vessel density; CVD: Capillary vessel density; NS: Nasal superior; RNFL: Retinal nerve fiber layer.

Table 3 Correlation analysis between RNFL's thickness and ONH morphological parameters

RNFL	VD		CVD	
	r	P	r	P
2-4 mm	0.141	0.240	0.175	0.145
S	-0.051	0.671	0.024	0.841
I	0.163	0.174	0.189	0.115
NS	0.233	0.05	0.288	0.015
NI	0.179	0.135	0.187	0.118
IN	0.021	0.865	0.080	0.507
IT	0.051	0.670	-0.040	0.738
TI	0.169	0.159	0.237	0.047
TS	0.221	0.064	0.004	0.976
ST	0.002	0.988	-0.074	0.540
SN	-0.111	0.356	-0.126	0.294

VD: Vessel density; CVD: Capillary vessel density; S: Superior; I: Inferior; NS: Nasal superior; NI: Nasal inferior; IN: Inferior nasal; IT: Inferior temporal; TI: Temporal inferior; TS: Temporal superior; ST: Superior temporal; SN: Superior nasal.

Garway-Heath et al[16] produced a clinically useful map that related the visual field test points to ONH regions. The map in this analysis was asymmetric, representing the location of the ONH above the horizontal meridian. Paracentral and arcuate regions of the visual field are defined by sectors in proximity to the poles of the ONH in the map. Subsequently, a peripapillary RNFL thickness map was used in the study by Tan et al[18]. to derive nerve fiber trajectories in the peripapillary region, and an over nerve fiber tracking algorithm was presented. The study devised a system to construct the NFF map and quantify it by track and sector in any test subject. On peripapillary OCT scans, the NFF tracks and sectors matched the typical nerve fiber trajectory over a wide area, potentially allowing efficient detection of focal damage and precise quantification of regional loss[18]. Therefore, in the current study, the measurement based on the ONH topographic map accurately detected the neural and vascular structural changes in early DR.

Diabetic microangiopathy is also known as retinal ischemia. One of the lesions in early DR, retinal capillary damage, is not fully formed into a local, visible non-perfusion region but manifests as decreased retinal blood flow density (RVD). It also found that the RVD of eyes with severe NPDR and PDR were significantly lower than those with mild NPDR and the normal control group, and the RVD of the eyes with DME was more significantly reduced[19]. In the eyes of NPDR without DME, the RVD decreased significantly with the severity of the disease[20]. Decreased VD in patients with non-DR and mild DR indicated a loss of papillary or lack of perfusion in the early stages of the disease[21]. In diabetic patients without DR, the superficial and deep decreased compared to healthy participants[22]. Li et al[23] analyzed the VD of 97 DM

patients and 48 controls and found that VD was decreased in the diabetic patient group. According to the anatomy, the capillaries in the inner layer of the retina are continuously branched from the central retinal artery that runs from the center of the optic disc. The retinal capillaries are distributed in layers, with the thickest next to the optic disc. Thus, it is speculated that when the retinal ischemic disease shows decreased RVD in the macular area at the end of the blood supply, the peripapillary blood supply should also decrease. The present study demonstrated that the peripapillary VD in diabetic patients decreased, and after removing the influencing factors of large blood vessels, CVD was also decreased.

These results were in line with the above theoretical speculation, i.e., the VD in the mild-moderate DR was significantly lower than in the normal control group, thereby suggesting that clinical examination should focus on whether the VD of DM patients can detect meaningful ischemic manifestations at the early stage.

When the large retinal vessels around the disc were removed, we found that in the ST area, the peripapillary CVD and RNFL thickness in the mild-moderate NPDR group was lower than that in the normal group, indicating a positive correlation. From an anatomical point of view, the macular area and the surrounding retina converge toward the optic disc in arcs on the upper and lower sides of the macular optic disc axis, and hence, the optic nerve and blood vessels in the supratemporal and infratemporal positions of the optic disc are denser than those in other parts[24]. After removing the large blood vessels, the changes in blood flow around the supply disc were observed accurately, and significant changes were detected in the blood vessels and nerves around the optic disc of DR, which were investigated further.

The superficial capillary layer at the optic disc, especially the radial peripapillary capillaries (RPC) blood vessels, run parallel to the direction of the nerve axons. The blood vessels are straight and lacking a large amount of intervascular anastomosis; also, the tolerance to hypoxia and injury was poor. However, the dense nerves in the superior and IT quadrants lead to high oxygen demand, thereby effectuating the cause of structural changes in the optic nerve that is susceptible to hyperglycemia[25].

The current results do not show how the progression of DR (DME and PDR) affects the peripapillary VD. Since macular edema distorts OCTA segmentation (which is critical for accurate measurements) and falsely increases peripapillary RNFL thickness, these factors are pre-specified as exclusion criteria[26]. In addition, panretinal photocoagulation and focal laser therapy are linked to declining RNFL thickness independently[27-29]. Therefore, if we recruited such patients, we would introduce uncontrollable confusion.

Nevertheless, the present study has a few limitations. First, this was a cross-sectional observational study. Thus, the association between improvements in peripapillary VD and development in the early-stage DR could be explained by longitudinal analysis. Second, the sample size was limited and insignificant to draw reasonable conclusions. Third, with the built-in program of the computer, we analyzed the microvasculature using a 4×4 mm^2 scan pattern. The RPC that supplies an RNFL blood flow extends to 8 mm from the optical disk temporal tip. Thus, a wide area for scanning the modifications of the VD could be useful[30].

In conclusion, the measurement based on the ONH topographic map may be more accurate than the traditional four-classification method. The peripapillary VD, CVD, and RNFL decreased in early DR, the changes in RNFL thickness were correlated with the CVD and/or VD in some regions. The current study provides mechanistic insight into DR, demonstrating functional and structural impairments around the optic disc in early DR and a correlation between these conditions. Furthermore, to validate the usefulness of peripapillary outcomes as biomarkers of early DR, longitudinal studies are warranted.

ACKNOWLEDGEMENTS

Conflicts of Interest: Wang XN, None; **Cai X,** None; **Li TT,** None; **Long D,** None; **Wu Q,** None.

REFERENCES

1 Lee R, Wong TY, Sabanayagam C. Epidemiology of diabetic retinopathy, diabetic macular edema and related vision loss. *Eye Vis* (*Lond*) 2015;2:17.

2 Olafsdottir E, Andersson DK, Dedorsson I, Svardsudd K, Jansson SP, Stefansson E. Early detection of type 2 diabetes mellitus and screening for retinopathy are associated with reduced prevalence and severity of retinopathy. *Acta Ophthalmol* 2016;94(3): 232-239.

3 Kim K, Kim ES, Yu SY. Longitudinal relationship between retinal diabetic neurodegeneration and progression of diabetic retinopathy in patients with type 2 diabetes. *Am J Ophthalmol* 2018;196:165-172.

4 Duh EJ, Sun JK, Stitt AW. Diabetic retinopathy: current understanding, mechanisms, and treatment strategies. *JCI Insight* 2017;2(14):e93751.

5 Simó R, Stitt AW, Gardner TW. Neurodegeneration in diabetic retinopathy: does it really matter? *Diabetologia* 2018;61(9):1902-1912.

6 Antonetti DA, Klein R, Gardner TW. Diabetic retinopathy. *N Engl J Med* 2012;366(13):1227-1239.

7 Nian S, Lo ACY, Mi YJ, Ren K, Yang D. Neurovascular unit in diabetic retinopathy: pathophysiological roles and potential therapeutical targets. *Eye Vis* (*Lond*) 2021;8(1):15.

8 Gardner TW, Davila JR. The neurovascular unit and the pathophysiologic basis of diabetic retinopathy. *Graefes Arch Clin Exp Ophthalmol* 2017;255(1):1-6.

9 Simó R, Simó-Servat O, Bogdanov P, Hernández C. Neurovascular unit: a new target for treating early stages of diabetic retinopathy. *Pharmaceutics* 2021;13(8):1320.

10 Yang JH, Kwak HW, Kim TG, Han JS, Moon SW, Yu SY. Retinal neurodegeneration in type II diabetic otsuka long-Evans tokushima fatty rats. *Invest Ophthalmol Vis Sci* 2013;54(6):3844-3851.

11 Li ST, Wang XN, Du XH, Wu Q. Comparison of spectral-domain optical coherence tomography for intra-retinal layers thickness measurements between healthy and diabetic eyes among Chinese adults. *PLoS One* 2017;12(5):e0177515.

12 Altmann C, Schmidt MHH. The role of microglia in diabetic retinopathy: inflammation, microvasculature defects and neurodegeneration. *Int J Mol Sci* 2018;19(1):E110.

13 Spaide RF, Klancnik JM Jr, Cooney MJ. Retinal vascular layers imaged by fluorescein angiography and optical coherence tomography angiography. *JAMA Ophthalmol* 2015;133(1):45-50.

14 Spaide RF, Fujimoto JG, Waheed NK, Sadda SR, Staurenghi G. Optical coherence tomography angiography. *Prog Retin Eye Res* 2018;64:1-55.

15 Vujosevic S, Muraca A, Gatti V, Masoero L, Brambilla M, Cannillo B, Villani E, Nucci P, De Cillà S. Peripapillary microvascular and neural changes in diabetes mellitus: an OCT-angiography study. *Invest Ophthalmol Vis Sci* 2018;59(12):5074-5081.

16 Garway-Heath DF, Poinoosawmy D, Fitzke FW, Hitchings RA. Mapping the visual field to the optic disc in normal tension glaucoma eyes. *Ophthalmology* 2000:107(10): 1809-1815.

17 Wilkinson CP, Ferris FL III, Klein RE, Lee PP, Agardh CD, Davis M, Dills D, Kampik A, Pararajasegaram R, Verdaguer JT,. Proposed international clinical diabetic retinopathy and diabetic macular edema disease severity scales. *Ophthalmology* 2003;110(9):1677-1682.

18 Tan O, Liu L, Liu L, Huang D. Nerve fiber flux analysis using wide-field swept-source optical coherence tomography. *Transl Vis Sci Technol* 2018;7(1):16.

19 Kim AY, Chu ZD, Shahidzadeh A, Wang RK, Puliafito CA, Kashani AH. Quantifying microvascular density and morphology in diabetic retinopathy using spectral-domain optical coherence tomography angiography. *Invest Ophthalmol Vis Sci* 2016;57(9):OCT362-OCT370.

20 Sambhav K, Abu-Amero KK, Chalam KV. Deep capillary macular perfusion indices obtained with OCT angiography correlate with degree of nonproliferative diabetic retinopathy. *Eur J Ophthalmol* 2017;27(6):716-729.

21 Forte R, Haulani H, Jürgens I. Quantitative and qualitative analysis of the three capillary plexuses and choriocapillaris in patients with type 1 and type 2 diabetes mellitus without clinical signs of diabetic retinopathy: a prospective pilot study. *Retina* 2020;40(2):333-344.

22 Dimitrova G, Chihara E, Takahashi H, Amano H, Okazaki K. Quantitative retinal optical coherence tomography angiography in patients with diabetes without diabetic retinopathy. *Invest Ophthalmol Vis Sci* 2017;58(1):190-196.

23 Li ZJ, Alzogool M, Xiao JH, Zhang S, Zeng P, Lan YQ. Optical

coherence tomography angiography findings of neurovascular changes in type 2 diabetes mellitus patients without clinical diabetic retinopathy. *Acta Diabetol* 2018;55(10):1075-1082.

24 Yu PK, Balaratnasingam C, Xu J, Morgan WH, *et al.* Label-free density measurements of radial peripapillary capillaries in the human retina. *PLoS One* 2015;10(8):e0135151.

25 Campbell JP, Zhang M, Hwang TS, Bailey ST, Wilson DJ, Jia Y, Huang D. Detailed vascular anatomy of the human retina by projection-resolved optical coherence tomography angiography. *Sci Rep* 2017;7:42201.

26 Yang HS, Woo JE, Kim MH, Kim DY, Yoon YH. Co-evaluation of peripapillary RNFL thickness and retinal thickness in patients with diabetic macular edema: RNFL misinterpretation and its adjustment. *PLoS One* 2017;12(1):e0170341.

27 Lee HJ, Kang TS, Kwak BS, Jo YJ, Kim JY. Long-term effect of panretinal photocoagulation on spectral domain optical coherence tomography measurements in diabetic retinopathy. *Curr Eye Res* 2017;42(8):1169-1173.

28 Huang T, Li XL, Xie J, Zhang L, Zhang GR, Zhang AP, Chen XT, Cui Y, Meng QL. Long-term retinal neurovascular and choroidal changes after panretinal photocoagulation in diabetic retinopathy. *Front Med* (*Lausanne*) 2021;8:752538.

29 Reddy SV, Husain D. Panretinal photocoagulation: a review of complications. *Semin Ophthalmol* 2018;33(1):83-88.

30 Mammo Z, Heisler M, Balaratnasingam C, *et al.* Quantitative optical coherence tomography angiography of radial peripapillary capillaries in glaucoma, glaucoma suspect, and normal eyes. *Am J Ophthalmol* 2016;170:41-49.